

INFLUENCE OF DETECTOR SELECTION ON BEAM PROFILE MEASUREMENT AND PERCENTAGE DEPTH DOSE IN SMALL-FIELD ^{60}Co RADIOTHERAPY

T. Akhter¹, M.S. Rahman², H.M. Jamil², S.S. Rubai¹, T. Siddiqua², M.H. Haque², B.N. Sattar², AKM M.H. Meaze^{1,3}

¹ Department of Physics, University of Chittagong, Chittagong, Bangladesh

² Secondary Standard Dosimetry Laboratory, Bangladesh Atomic Energy Commission, Savar, Dhaka, Bangladesh

³ Faculty of Natural Sciences, Asian University for Women, Chittagong, Bangladesh

Abstract— Modern technological developments have greatly improved ^{60}Co systems by providing multi-leaf collimators (MLC). These advancements have rendered these systems appropriate for use in modern medicine, providing more accurate and potent therapeutic alternatives. The aim of this study is to assess the dosimetric parameters such as symmetry, flatness, and penumbra of beam profiles, and percentage depth dose (PDD) in small fields of ^{60}Co teletherapy beam (Theratron Equinox External Beam Therapy System) by using four different detectors, which are Semiflex chamber, Pinpoint chamber, Diode detector, and Microdiamond detector. The measurements were performed in a 3D water phantom known as Blue Phantom² in a reference field size of $10 \times 10 \text{ cm}^2$, and in small field sizes of 5×5 , 4×4 , 3.5×3.5 , 3×3 , 2.5×2.5 , and $2 \times 2 \text{ cm}^2$. The code of practice of the American Association of Physicists in Medicine (AAPM) Radiation Therapy Task Group No. 45 was followed to examine beam profiles. Among all of these detectors, Semiflex and Microdiamond detectors express more reasonable responses for the analysis of beam profiles. In terms of accurate penumbra measurement, the Microdiamond detector is advantageous. Comparing with the values of British Journal of Radiology (BJR) supplement 25, Microdiamond is the best fit for PDD measurements. The analysis would be helpful in defining future protocols for the development of small field dosimetry.

Keywords— ^{60}Co Teletherapy Beam, Small Field Dosimetry, Beam Profile, Percentage Depth Dose, Microdiamond Solid-State Detector.

I. INTRODUCTION

The ^{60}Co unit has a long history of usage in cancer therapy, and it is currently used in conventional radiation therapy for both radical and palliative treatments. Machines with ^{60}Co require less technical skill to operate and require less maintenance [1]. ^{60}Co teletherapy, a high-energy photon beam radiation treatment, is suitable for difficult superficial anatomic locations and can reduce radiation toxicity in the proximate organ at risk volume. Treatment automation can be facilitated by integrating technology like multi-leaf collimators in ^{60}Co teletherapy devices. It's crucial for medical physicists to consider ^{60}Co teletherapy's role in advanced technologies like IMRT. ^{60}Co based radiation treatment is still widely used in developed nations as well as poor nations with severely restricted access to

radiation therapy [2]. Radiation oncologists recommend radiation therapy doses to treat or control illnesses with minimal damage to healthy tissues. Accurate dosage delivery relies on precise source dosimetry, and the International Commission on Radiation Units and Measurement advises that dosages should be within $\pm 5\%$ of the recommended dose, as the process involves combining multiple tasks for effective treatment [3].

In general, small fields correspond with therapeutic field sizes, which range from 4×4 to $0.3 \times 0.3 \text{ cm}^2$. While both large and small therapeutic fields are significant from a therapeutic perspective, small therapeutic fields are more significant in certain circumstances, particularly when it comes to head and neck tumors, because organs at risk are situated inside the treatment volume. In small fields, however, the effects of the collimators' scattering radiation are more significant. Furthermore, at the boundary of the treatment domains, the penumbra effect is a significant factor. In order to obtain more precise dosimetry of such fields, it is anticipated that this effect will be as small as feasible [4]. Applying small fields that are either static or dynamic is essential with the advent of new procedures like volumetric modulated radiation therapy (VMAT), intensity modulated radiation therapy (IMRT), stereotactic body radiotherapy (SBRT), and stereotactic radiosurgery (SRS). Numerous advancements in treatment equipment have been made specifically for this purpose. Small field dosimetry presents a number of difficulties, such as the radiation field's steep gradient, the volume averaging effect, the lack of charged particle equilibrium, the partial occlusion of the radiation source, beam alignment, and the inability to utilize a reference dosimeter. Owing to these difficulties, small field dosimetry calls for specialized dosimeters. To accurately acquire the beam profile in high gradient dosage locations, like small fields, high spatial resolution detectors must be used [5].

Bayatiani *et al.* [6] examined the symmetry and flatness achieved with three distinct dosimeters for varied small and large fields in electron beam radiation with linac. According to their findings, there are slight discrepancies in the reactions of different dosimeters (Diode E detector, Semiflex-3D, and Advanced Markus ionization chambers) in the detection of electron beam symmetry and flatness.

For small and large field sizes, the symmetry and flatness values rise with increasing field size and electron beam energy, while the increases are slight in some circumstances. Platoni *et al.* [7] analyzed and compared data for penumbra size, flatness, and symmetry using six different measurement techniques. The results show that determining penumbra size is highly reliant on the measuring system. For photon measurements, the diodes had the smallest penumbra, followed by the LA48, and the Semiflex had the largest penumbra. Harzani *et al.* [8] analyzed and compared the dosimetric features of two small detectors (Semiflex®3D and microdiamond) in small field relative dosimetry. The results show that both studied detectors worked well in small field relative dosimetry, and that the microdiamond detector is preferable for detecting penumbra. Woodings *et al.* [9] characterized the influence of the PTW 60019 Microdiamond on a magnetic resonance linac (MRI-linac). Because of its tiny physical size, good signal-to-noise ratio, and approaching water equivalency, the PTW 60019 Microdiamond is close to an ideal detector for small field dosimetry. Marinelli *et al.* [10] examined for the first time the dosimetric characteristics of a recently developed commercial synthetic diamond detector (PTW Microdiamond) using high-energy scanning clinical carbon ion beams produced by a synchrotron at the Italian National Center for Oncological Hadron Therapy (CNAO) facility. With negligible LET and dose-rate dependence, the study's findings demonstrated that this detector is appropriate for clinical carbon ion beam dosimetry.

For radiation therapy to produce satisfactory treatment results, quality control is essential. As part of quality control, the dosimetric performance of radiation detectors must be appropriately and precisely evaluated. The objective of the present study is to evaluate the dosimetric performance for the different types of detectors (Semiflex chamber type 31010, Pinpoint 3D chamber type 31022, Diode E detector type 60017, and Microdiamond detector

type 60019) in small fields of ^{60}Co teletherapy beam. The dosimetric parameters symmetry, flatness, and penumbra of ^{60}Co gamma beam profiles, and percentage depth dose (PDD), were investigated for a reference field size of $10 \times 10 \text{ cm}^2$, and for small field sizes of 5×5 , 4×4 , 3.5×3.5 , 3×3 , 2.5×2.5 , and $2 \times 2 \text{ cm}^2$. The measurements were conducted in a Blue Phantom² 3D water phantom. Beam profiles were investigated using the code of practice of the American Association of Physicists in Medicine Radiation Therapy Task Group No. 45.

II. MATERIALS AND METHODS

The experimental procedure was performed by using AAPM TG 45 code of practice for radiotherapy at the ^{60}Co Gamma Lab, Secondary Standard Dosimetry Laboratory (SSDL), Bangladesh Atomic Energy Commission (BAEC), Savar, Dhaka, Bangladesh. The irradiations were performed by Theratron Equinox External Beam Therapy System (^{60}Co Teletherapy Unit, Best Theratronics Ltd., Ottawa, Ontario, Canada). PDD measurement, and beam profile analysis have been investigated for four detectors, Semiflex chamber type 31010, Pinpoint 3D chamber type 31022, Diode E detector type 60017, and Microdiamond detector type 60019 (PTW, Freiburg, Germany) in a reference field size of $10 \times 10 \text{ cm}^2$, and in small field sizes of 5×5 , 4×4 , 3.5×3.5 , 3×3 , 2.5×2.5 , and $2 \times 2 \text{ cm}^2$. The measurements were performed in a 3D water phantom known as Blue Phantom² (IBA Schwarzenbruck, Germany). A phantom is a mass of material similar to human tissue used to investigate the effect of radiation beams on humans. The doses have been scanned using common control unit (CCU) which is close-packed unit completely software controlled combining controller and electrometers. Several features of the detectors used in this study are presented in Table 1.

Table 1: Technical specifications of the different detectors used in this work

Specifications	Semiflex Chamber Type 31010	Pinpoint 3D Chamber Type 31022	Diode E Detector Type 60017	Micro diamond Detector Type 60019
Type of product	vented cylindrical ionization chamber	vented cylindrical ionization chamber	p-type silicon diode	synthetic single crystal diamond detector
Direction of incidence	radial	radial, axial	axial	axial
Nominal sensitive volume	0.125 cm^3	0.016 cm^3	0.030 mm^3	0.004 mm^3
Reference point	on chamber axis, 4.5 mm from chamber tip	on chamber axis, 2.4 mm from chamber tip	on detector axis, 1.33 mm from detector tip	on detector axis, 1 mm from detector tip
Chamber voltage	+400 V nominal	+300 V nominal	0 V	0 V
Field size	$3 \times 3 \text{ cm}^2 \dots 40 \times 40 \text{ cm}^2$	$2 \times 2 \text{ cm}^2 \dots 40 \times 40 \text{ cm}^2$	$1 \times 1 \text{ cm}^2 \dots 10 \times 10 \text{ cm}^2$	$1 \times 1 \text{ cm}^2 \dots 40 \times 40 \text{ cm}^2$

Normally, it is described for several gantry angles, a specific depth in a phantom, multiple field sizes, and both transverse directions of collimator motion. Flatness can be specified as a maximum permissible percentage variation from the average dose across the central 80% of the FWHM of the profile in a plane transverse to the beam axis. That is, the flatness F is given by,

$$F = \frac{D_{\max} - D_{\min}}{D_{\max} + D_{\min}} \times 100\% \quad (1)$$

Where D_{\max} and D_{\min} are the maximum and minimum dose values in the central 80% of the profile.

It is usually specified for one or more field sizes, for a particular depth in a phantom, and for several gantry angles. Typically, a dosimetry scanning device is used for evaluating symmetry and flatness in a water phantom. The lateral distance on one side of a beam profile between the 80% and 20% of maximum dosage locations is known as the penumbra [11]. The dosage for a ^{60}Co beam is highest in the central beam axis and is smaller as it gets closer to the beam edges. The dosage rapidly decreases with lateral distance from the beam central axis in the penumbra region at the beam edges. The dose falloff around the geometric beam edge is sigmoid in shape and extends into the penumbral tail region under the collimator jaws. In this region, there is a small dose component attributed to transmission through the collimator jaws (transmission penumbra), a significant dose component attributed to in-patient radiation scatter (scatter penumbra), and a component attributed to finite source size (geometric penumbra) [12].

The dosage at any depth along the central axis of the radiation beam, also known as the percentage depth dose (PDD), is one of the most often used quantities in dosimetry. The PDD is defined by:

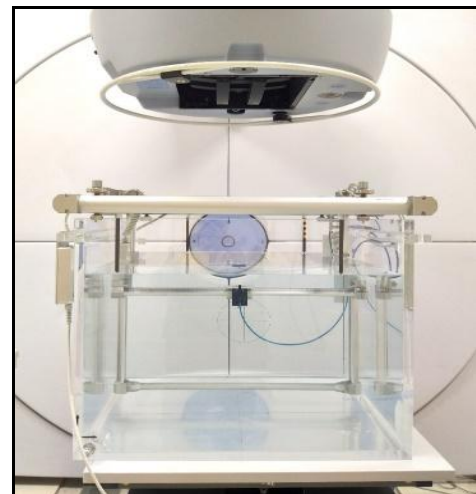
$$PDD = \frac{\text{Dose at any depth along central axis}}{\text{Dose at depth of maximum dose along central axis}} \times 100\% \quad (2)$$

PDD diminishes with increasing measurement depth (except in the buildup region). This results from the photon beam's exponential attenuation as it travels through the body. PDD rises with increasing field size. This is the result of higher dispersion due to the larger collimator and the irradiated patient area [13].

For beam profiles, the measurements were performed with SSD at 100 cm and at a reference depth of 5 g/cm². Using CCU, the doses have been scanned at a rate of 0.3 cm/sec in the cross-line direction and an output step width of 0.12 cm. Data analysis of the scanned relative doses has been performed using the AAPM TG 45 protocol for measurement of symmetry, flatness, and penumbra. For the measurement of PDD, scanned doses have been taken using the continuous mode of gamma beam radiation. Using CCU, the doses have been scanned at a rate of 0.3 cm/sec at several depths (from -0.05 cm to 20 cm) with an output step width of 0.12 cm, and equation (2) is employed to measure PDD. The direction of incidence of the chambers is radial, and that of the solid-state detectors is axial. In Figure 1, a typical set-up for the measurements is presented. OriginPro 2024 and Microsoft Excel 2021 software were used for the analysis of scanned relative doses to measure symmetry deviation, flatness deviation, and penumbra of beam profiles and to measure PDD. OriginPro was used for graph plotting and statistical analysis. Microsoft Excel was used to organize the data and do exploratory computations.



(a)



(b)

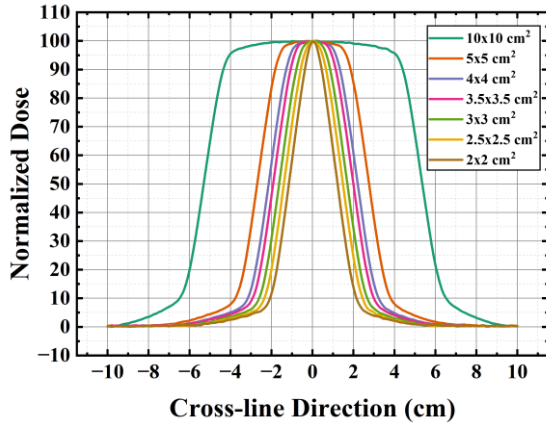
Figure 1: Set up of (a) Theratron Equinox External Beam Therapy System and (b) measurement for beam profile using Microdiamond detector at SSDL, BAEC, Savar, Dhaka, Bangladesh

III. RESULTS AND DISCUSSION

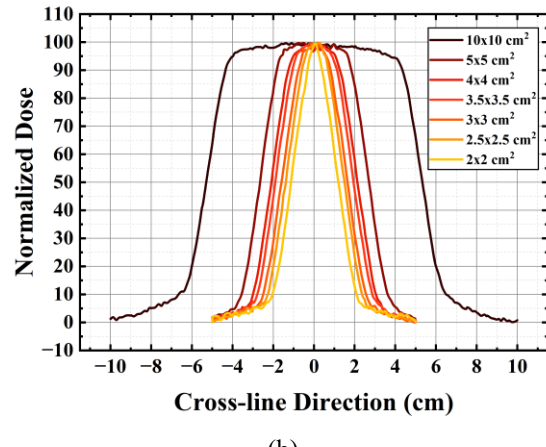
Beam Profiles

For a ^{60}Co beam the dose at any depth is largest on the central beam axis and then decreases towards the beam edges. Near the beam edges in the penumbra region the dose decreases rapidly with lateral distance from the beam central axis. Four beam profiles of ^{60}Co gamma radiation, as shown in Figure 2, were obtained using four detectors for the reference field size ($10 \times 10 \text{ cm}^2$) and small field sizes (5×5 , 4×4 , 3.5×3.5 , 3×3 , 2.5×2.5 and $2 \times 2 \text{ cm}^2$). Semiflex and Microdiamond detectors outperformed Pinpoint and Diode E detectors in terms of beam profile smoothness. Pinpoint responses were less reliable among all these detectors due to fluctuations in the beam profile measurements. Despite of Diode E responses for field sizes

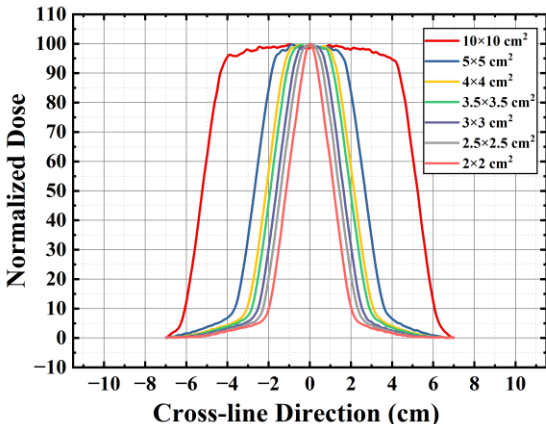
less than $4 \times 4 \text{ cm}^2$ are reasonable, for larger field sizes it is not recommended for dose profile measurements.



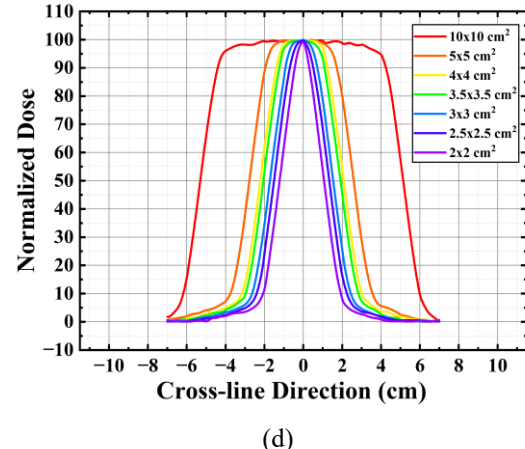
(a)



(b)



(c)



(d)

Figure 2: Beam profiles obtained using (a) Semiflex, (b) Pinpoint, (c) Diode E, and (d) Microdiamond for different field sizes.

Table 2: Results of symmetry deviation, flatness deviation and penumbra obtained from Semiflex detector

Field Size (cm^2)	Symmetry Deviation (%)	Flatness Deviation (%)	Penumbra Left-Side (mm)
Reference	10x10	0.21	2
	5x5	0.37	9
	4x4	0.78	13
	3.5x3.5	0.98	13
	3x3	1.47	16
	2.5x2.5	2.14	17
	2x2	2.46	18
	0.21 – 2.46	2 – 18	13.33 – 11.51

Table 3: Results of symmetry deviation, flatness deviation and penumbra obtained from Pinpoint detector

Field Size (cm^2)	Symmetry Deviation (%)	Flatness Deviation (%)	Penumbra Left-Side (mm)
Reference	10x10	0.87	3
	5x5	1.02	10
	4x4	0.83	13
	3.5x3.5	1.18	14
	3x3	1.49	17
	2.5x2.5	3.23	17
	2x2	3.04	19
	0.83 – 3.23	3 – 19	13.53 – 11.84

Symmetry deviation, flatness deviation, and penumbra values of beam profiles for Semiflex, Pinpoint, Diode E and Microdiamond are shown in Tables 2, 3, 4, and 5, respectively. The difference between the maximum and minimum doses grows in the plateau region of beam profiles when field sizes are reduced. As a result, the flatness deviation increases with field size reduction. Penumbra values decrease as field size decreases due to fewer photons dispersed on the collimator's edge. The deviation ranges for symmetry and flatness are (0.21–2.46)

% and (2–18) %, respectively, and the penumbra range is (13.33–11.51) mm obtained using the Semiflex detector, as represented in Table 2. For Pinpoint, as shown in Table 3, the deviation ranges for symmetry and flatness are (0.83–3.23) % and (3–19) % respectively. Penumbra values fluctuate as field size decreases due to the size and shape of the ionization chamber, and the range is (13.53–11.84) mm. For Diode E, as presented in Table 4, the deviation ranges for symmetry and flatness are (0.49–0.96) % and (3–18) % respectively. Penumbra values decrease as field size decreases, but in this case, for field size $10 \times 10 \text{ cm}^2$, the penumbra value is less than the value for field size $5 \times 5 \text{ cm}^2$, and the range is (11.94–11.44) mm. Diode E has limitations that does not respond properly to larger field sizes. For Microdiamond, as shown in Table 5, the deviation ranges for symmetry and flatness are (0.61–5.49) % and (3–22) % respectively. Penumbra values decrease as field size decreases, and the range is (12.00–11.31) mm.

Table 4: Results of symmetry deviation, flatness deviation and penumbra obtained from Diode E detector

Field Size (cm^2)	Symmetry Deviation (%)	Flatness Deviation (%)	Penumbra Left-Side (mm)
Reference	10×10	0.54	3
	5×5	0.58	11.94
	4×4	0.56	11.80
	3.5×3.5	0.79	11.82
	3×3	0.52	11.57
	2.5×2.5	0.49	11.45
	2×2	0.96	11.44
Range	0.49 – 0.96	3 – 18	11.94 – 11.44

Table 5: Results of symmetry deviation, flatness deviation and penumbra obtained from Microdiamond detector

Field Size (cm^2)	Symmetry Deviation (%)	Flatness Deviation (%)	Penumbra Left-Side (mm)
Reference	10×10	0.61	3
	5×5	2.06	11.79
	4×4	2.22	11.76
	3.5×3.5	2.56	11.52
	3×3	4.10	11.69
	2.5×2.5	4.88	11.31
	2×2	5.49	11.34
Range	0.61 – 5.49	3 – 22	12.00 – 11.31

Among all of these detectors, Semiflex and Microdiamond detectors express more reasonable responses that symmetry is decreasing with respect to the decrease in field sizes. It is explicitly stated for every detector that the beam profile is flatter at larger field sizes than it is at smaller field sizes. It can be concluded that Pinpoint responses are unreliable for measuring the penumbra of beam profiles. In this case, it is advised against using Diode E to assess the beam profiles for larger field sizes. Microdiamond solid-state detector responses are more

genuine than Semiflex ionization chamber, due to the volume effect, Semiflex overestimates the breadth of the penumbra.

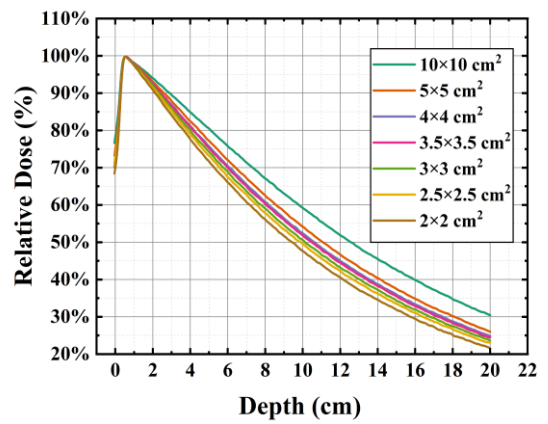
Percentage Depth Dose

The maximum dose of the photon beam on the small field area is achieved at depth, D_{max} . The percentage depth dose (beyond the depth of the maximum dose) decreases with depth. Due to the fixed SSD, the source-to-detector distance will increase with increasing depth. PDD changes with depth due to buildup, attenuation, and distance (inverse square factor) [14]. The PDD curves of ^{60}Co gamma radiation, as represented in Figure 3, were obtained using four detectors for the reference field size ($10 \times 10 \text{ cm}^2$) and small field sizes (5×5 , 4×4 , 3.5×3.5 , 3×3 , 2.5×2.5 , and $2 \times 2 \text{ cm}^2$). PDD declines with the reduction of field sizes. For different field sizes, the maximum dose peak almost intersects at the same point for all of these detectors.

According to Table 6, D_{max} varies from 0.52 to 0.53 cm for Semiflex and from 0.41 to 0.66 cm for Pinpoint. For Diode E, it is found at a fixed point of 0.58 cm for a variety of field sizes. D_{max} for Microdiamond does not change when field sizes are changed from large to small, and the number 0.53 cm is more consistent with the value supplied by the BJR supplement, 25, which is 0.5 cm depth [15]. It is inadvisable not to use Pinpoint for PDD calculation due to fluctuations in measurements.

Table 6: Position of 100% PDD for Different Detectors, D_{max} (cm)

Field Size (cm^2)	Semiflex Chamber Type 31010	Pinpoint 3D Chamber Type 31022	Diode E Detector Type 60017	Microdiamond Detector Type 60019
10×10	0.52	0.41	0.58	0.53
5×5	0.52	0.49	0.58	0.53
4×4	0.53	0.66	0.58	0.53
3.5×3.5	0.53	0.49	0.58	0.53
3×3	0.52	0.51	0.58	0.53
2.5×2.5	0.52	0.49	0.58	0.53
2×2	0.53	0.61	0.58	0.53



(a)

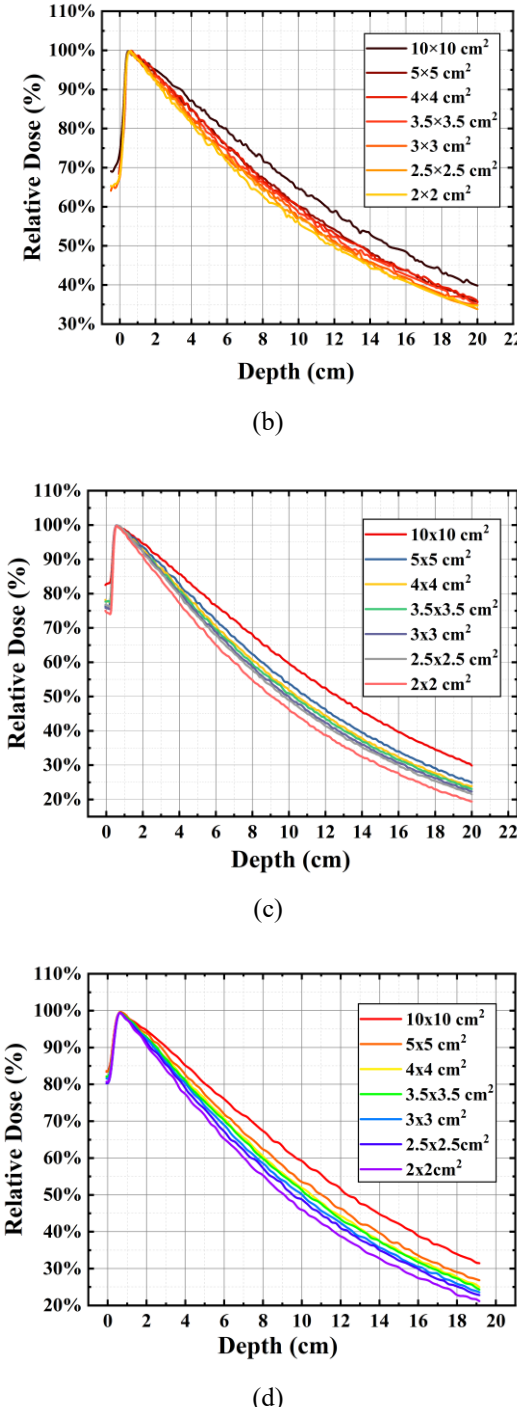


Figure 3: PDD curves obtained using (a) Semiflex, (b) Pinpoint, (c) Diode E, and (d) Microdiamond for different field sizes

From Table 7, it can be determined which detector is optimal for PDD measurement in the reference depth (z_{ref}). PDD declines with the reduction of field sizes in the reference depth (z_{ref}) for all detectors. Pinpoint does not respond linearly, and PDD values vary significantly within a $5 \times 5 \text{ cm}^2$ to $3.5 \times 3.5 \text{ cm}^2$ field area. There is excellent

linearity in the responses of PDD measurement with respect to reductions in field sizes in reference depth for Semiflex, Diode E, and Microdiamond. PDD value at reference depth is 80.4% for reference field size $10 \times 10 \text{ cm}^2$ and at SSD 100 cm, according to BJR supplement 25 [15]. Considering this supplement as standard, Microdiamond is the best fit for PDD measurements over Semiflex and Diode E.

Table 7: PDD (%) at Reference Depth (z_{ref}) for Different Detectors, PDD (z_{ref})%

Field Size (cm ²)	Semiflex Chamber Type 31010	Pinpoint 3D Chamber Type 31022	Diode E Detector Type 60017	Microdiamond Detector Type 60019
10×10	80.59	82.68	81.04	80.44
5×5	77.29	79.66	76.99	77.55
4×4	75.69	80.29	76.08	76.59
3.5×3.5	75.35	78.71	74.88	75.69
3×3	74.31	77.45	74.13	74.46
2.5×2.5	73.17	77.03	73.23	73.66
2×2	71.78	75.78	70.86	72.05

IV. CONCLUSION

This study's goal is to assess the dosimetric performance for Semiflex chamber type 31010, Pinpoint 3D chamber type 31022, Diode E detector type 60017, and Microdiamond detector type 60019 in small field of ^{60}Co teletherapy beam. The dosimetric parameters symmetry, flatness, and penumbra of ^{60}Co gamma beam profiles, and PDD, were investigated for a reference field size of $10 \times 10 \text{ cm}^2$ and for small field sizes of 5×5 , 4×4 , 3.5×3.5 , 3×3 , 2.5×2.5 , and $2 \times 2 \text{ cm}^2$. A Blue Phantom² 3D water phantom was used for the measurements. The code of practice of the American Association of Physicists in Medicine (AAPM) Radiation Therapy Task Group No. 45 was followed to examine beam profiles. Following extensive experimental investigations, the use of a Microdiamond solid-state detector for small field dosimetry analysis in ^{60}Co teletherapy beams is strongly recommended due to its small sensitive volume, flat energy response, compact size, high sensitivity, and resistance to radiation damage. The analysis would be helpful in defining future protocols for the development of small-field dosimetry.

V. ACKNOWLEDGMENTS

The authors would like to express their sincere thanks to the staff and scientists of the Secondary Standard Dosimetry Laboratory of the Bangladesh Atomic Energy Commission for their strong support in conducting this research. The administrative assistance for this research work was provided by the ADP project "Establishment of Calibration and Quality Control Facilities for Radiotherapy, Diagnostic Radiology, and Neutron" by the Ministry of Science and Technology, Bangladesh.

REFERENCES

1. Singh A, Singh G, Saini A, Kinhikar RA, Kumar P., Small fields characterization of teletherapy cobalt-60 photon beam: An experimental and Monte-Carlo study. *Measurement: Sensors*. February 2023; 25:100595.
2. Mathuthu M, Mdziniso NW, Asres YH., Dosimetric evaluation of Cobalt-60 teletherapy in advanced radiation oncology: *Journal of Radiotherapy in Practice*. March 2019;18(1) : 88-92.
3. Baba MM, Mohib-ul-Haq M, Khan MA., Dosimetric consistency of Co-60 teletherapy unit-a ten years study, *International Journal of Health Sciences*. January 2013;7(1) : 15.
4. Aghayan SA, Nateghi N, Layegh M., Experimental validation of small-field dosimetry in radiotherapy using ionization chamber and edge detector, *Iranian Journal of Medical Physics*. May 2021;18(3) : 148-53.
5. Parwaie W, Refahi S, Ardekani MA, Farhood B., Different dosimeters/detectors used in small-field dosimetry, Pros and Cons. *Journal of Medical Signals & Sensors*. July 2018 ;8(3) : 195-203.
6. Bayatiani MR, Fallahi F, Aliasgharzadeh A, Ghorbani M, Khajetash B, Seif FA, Comparison of symmetry and flatness measurements in small electron fields by different dosimeters in electron beam radiotherapy. *Reports of Practical Oncology and Radiotherapy*. 2021;26(1) : 50-8.
7. Patatoukas GD, Kalavrezos P, Seimenis I, Dilvoi M, Kouloulias V, Efstatopoulos E, Platoni K., Determination of beam profile characteristics in radiation therapy using different dosimetric set ups., *Jbuon*. September 2018; 23(5) : 1448-59.
8. Harzani ZM, Larizadeh MH, Namiranian N, Nickfarjam A., Evaluation and comparison of dosimetric characteristics of semiflex® 3D and microdiamond in relative dosimetry under 6 and 15 MV photon beams in small fields. *Journal of Biomedical Physics & Engineering*. October 2022;12(5): 477.
9. Woodings SJ, Wolthaus JW, van Asselen B, De Vries JH, Kok JG, Lagendijk JJ, Raaymakers BW., Performance of a PTW 60019 microDiamond detector in a 1.5 T MRI-linac. *Physics in Medicine & Biology*. March 2018 ; 63(5) : 05NT04.
10. Marinelli M, Prestopino G, Verona C, Verona-Rinati G, Ciocca M, Mirandola A, Mairani A, Raffaele L, Magro G., Dosimetric characterization of a microDiamond detector in clinical scanned carbon ion beams. *Medical physics*. April 2015; 42(4) : 2085-93.
11. Biggs PJ, Ling CC, Purdy JA, van de Geijn J., AAPM code of practice for radiotherapy accelerators: report of AAPM Radiation Therapy Task Group No. 45. *Medical Physics*. July 1994; 21:1093.
12. Podgorsak EB. Radiation oncology physics: a handbook for teachers and students. 2005.
13. Murshed H, editor. Fundamentals of radiation oncology: physical, biological, and clinical aspects. Academic Press; January 2019.
14. Chang DS, Lasley FD, Das IJ, Mendonca MS, Dynlacht JR., Basic radiotherapy physics and biology. Springer International Publishing; September 2014.
15. McKenzie AL. Cobalt-60 gamma-ray beams. BJR supplement. 1996; 25 : 46-61.

Contacts of the corresponding author:

Author: M.S. Rahman
Institute: University of Chittagong
City: Chittagong
Country: Bangladesh
Email: shakilurssdl@baec.gov.bd